Two-phase scenario for the metal-insulator transition in colossal magnetoresistance manganites

A. Weiße,[1] J. Loos,[2] and H. Fehske[1]
[1]*Physikalisches Institut, Universität Bayreuth, 95440 Bayreuth, Germany*
[2]*Institute of Physics, Czech Academy of Sciences, 16200 Prague, Czech Republic*
(Received 16 January 2001; revised manuscript received 24 April 2001; published 21 August 2001)

Recent experiments indicate the coexistence of localized and itinerant charge carriers close to the metal-insulator transition in the ferromagnetic phase of colossal magnetoresistive manganese perovskites. For a theoretical description of the colossal magnetoresistance transition we propose a two-phase model of competing insulating polaronic and ferromagnetic metallic phases with equal hole densities. We find that the subtle balance between these two phases with distinctly different electronic properties can be readily influenced by varying physical parameters, producing various ''colossal'' effects, such as the large magnetization and conductivity changes in the vicinity of the transition temperature.

DOI: 10.1103/PhysRevB.64.104413 PACS number(s): 75.30.Vn, 71.38.Ht, 75.30.Kz, 71.10.−w

I. INTRODUCTION

The transition from a metallic ferromagnetic (FM) low-temperature phase to an insulating paramagnetic high-temperature phase observed in some hole-doped manganese oxides [such as the perovskite family $La_{1-x}(Sr,Ca)_xMnO_3$] is associated with an unusual dramatic change in their electronic and magnetic properties. This includes a spectacularly large negative magnetoresistive response to an applied magnetic field—sometimes termed colossal magnetoresistance (CMR)—which might have important technological applications.[1] Starting with the pioneer papers of Jonker and van Santen half a century ago,[2] this challenging behavior has stimulated a considerable amount of experimental and theoretical work,[3–5] however, much of the basic physics of the CMR still remains controversial.

Early studies on lanthanum manganites concentrated on the link between magnetic correlations and transport and attributed the low-T metallic behavior to Zener's *double-exchange mechanism*,[6–8] which maximizes the hopping of a strong Hund's rule coupled Mn e_g electron in a polarized background of the core spins (Mn t_{2g} electrons). The quantum version of this process has been described by Kubo and Ohata.[9] Although there is not much controversy about the qualitative validity of the double-exchange scenario to stabilize this FM ''Zener'' state, it has been argued that physics beyond the double-exchange scenario is important not only to explain the very complex phase diagram of the manganites[10,11] but also the CMR transition itself.[12,13] The difficulty is that magnetic scattering of itinerant charge carriers (doped holes) from enhanced fluctuations near T_c is the exclusive mechanism to drive the metal-insulator transition in the double-exchange-only models. However, even complete spin disorder does not lead to a significant reduction of the electronic bandwidth and therefore cannot account for the observed scattering rate[14–16] (cf. also the discussion in Refs. 17 and 18).

In view of this problem, it has been suggested that orbital[19–23] and, in particular, *lattice effects*[12,24–27] are crucial in explaining the CMR phenomenon. The argument was that the electron-lattice coupling is known to be strong in at least some members of the perovskite manganese family and tends to localize doped hole carriers as *small polarons* by changing the ratio of the energy gain through polaron formation to the conduction band kinetic energy.[14,28] Clearly this ratio is extremely sensitive to changes of the magnetic correlations by varying magnetic field, temperature, and carrier concentration.[14,28] There are two types of lattice distortions that are important in manganites. First the partially filled e_g states of the Mn^{3+} ion can be affected by Jahn-Teller distortions, i.e., the system can gain energy from a quadrupolar symmetric elongation of the oxygen octahedra that lifts the e_g degeneracy.[29,30] A second possible deformation is an isotropic shrinking of a MnO_6 octahedron. This ''breathing''-type distortion couples to changes in the e_g charge density, i.e., is always associated with the presence of a Mn^{4+} ion. In the lightly doped region of the phase diagram, holes are pinned onto Mn^{4+} sites by locally ''undoing'' the cooperative Jahn-Teller distortion, i.e., forming so-called ''anti Jahn-Teller polarons''.[31] As pointed out in a recent paper by Billinge *et al.*,[32] this perspective is not appropriate, or at least is misleading, in the heavily doped material, when the high-temperature polaronic state is approached from the FM metallic phase, because there are initially almost no Jahn-Teller-distorted octahedra. In this regime, both, breathing-mode collapsed (Mn^{4+}) *and* Jahn-Teller-distorted (Mn^{3+}) sites are created simultaneously when the holes are localized in passing the metal-insulator transition. To avoid any confusion, in what follows, we refer to a ''polaron'' as a doped charge carrier (hole) that is quasilocalized with an associated lattice distortion.[32] The relevance of small polaron transport above T_c is obvious from the activated behavior of the conductivity.[33] Consequently many theoretical studies focused on polaronic approaches.[15,34–39] Polaronic features have been established by a variety of experiments. For example, high-temperature thermopower[40,41] and Hall mobility measurements[42] confirmed the polaronic nature of charge carriers in the paramagnetic phase. More directly the existence of polarons has been demonstrated by atomic pair distribution,[43] x-ray, and neutron scattering studies.[44–46] Interestingly it seems that the charge carriers partly retain their polaronic character well *below* T_c, as proved, e.g., by neutron pair-distribution-function (PDF) analysis[47] and very recent resistivity measurements.[48] Moreover, there have been

 ©2001 The American Physical Society

predictions, based on x-ray-absorption fine-structure (XAFS) data,[49] that small octahedral distortions persist at low temperature, forming a nonuniform metallic state. Particularly striking in this respect is the direct relationship between the structural distortions and the magnetism of the CMR perovskites.[50] That means that even the nature of the FM low-temperature phase is not yet completely resolved. Obviously manganese oxides, above and below T_c, are in the subtle regime where many different tendencies are in competition and it seems that more refined ideas are needed to explain the main properties of these materials.

Realizing that *intrinsic inhomogeneities* and *mixed-phase characteristics* exist and might play a key role in manganites, two-phase models describing the coexistence and interplay of localized and itinerant carriers have recently attracted a lot of attention (for a review see Ref. 5). For example, *phase separation* scenarios involving phases with *different* electronic densities have been adopted to describe the mixed-phase tendencies in manganites.[13,51] These approaches are particularly meaningful in the limits of small ($x<0.1$) and high ($x\sim 1$) hole densities, where nanometer-scale coexisting clusters have been reported. In the CMR regime ($0.15<x<0.5$), however, several experiments reported clusters as large as micrometers in size.[52,53] Of course, such μm-sized domains, if charged, are energetically unstable because of the electroneutrality condition enforced by long-range Coulomb repulsion. Therefore an alternative concept, where the metal-insulator transition and the associated magnetoresistance behavior is viewed as a *percolation phenomenon*, was analyzed theoretically[54–56] and now has a substantial experimental support by pulsed neutron,[57] electron microscopy,[53] Mössbauer,[58] and scanning tunnel spectroscopy[52] studies.

Motivated by this situation, in the present work we propose an approach to the metal-insulator transition in manganites that takes into account the percolative coexistence of two ''intertwined'' *equal-density* phases: metallic double-exchange dominated and polaronic insulating. The transition is driven by a feedback effect that, at T_c, abruptly lowers the number of delocalized holes, i.e., conducting sites, leading to an collapse of the bandwidth of the Zener state. The physical picture behind our approach is corroborated by x-ray-XAFS,[50] PDF,[32] and neutron scattering data,[59] which indicate that charge-localized and -delocalized phases coexist close to the CMR transition. Further support comes from zero-field muon spin relaxation and neutron spin echo measurements,[60] reporting two time scales in the FM phase of $La_{1-x}Sr_xMnO_3$, where the more rapidly relaxing component has been attributed to spins inside the overlapping metallic region and the slower Mn-ion relaxation rate was associated with polarons that occupy a diminishing volume fraction as the temperature is lowered.

II. TWO-PHASE MODEL FOR THE CMR TRANSITION

To set up a two-component description of the metal-insulator transition in CMR manganites, let us first characterize the two competing phases. For the delocalized phase we assume that the conditions leading to the familiar double-exchange model are fulfilled. This means we consider the limit of large Coulomb and Hund's rule couplings and describe the e_g holes by a single band model, where the orbital dependency of the hopping enters via an effective band structure.[61] The insulating phase is modeled as built up by localized Jahn-Teller and breathing-type distortions, i.e., it is approximated by a band with negligible dispersion.

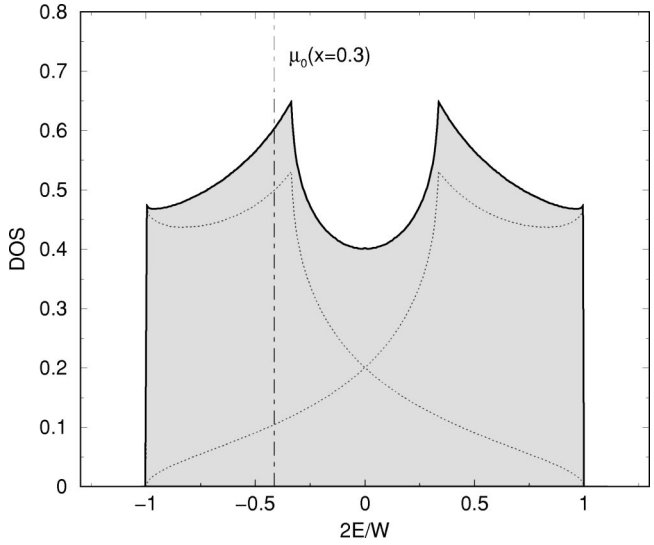

FIG. 1. Density of states corresponding to the band dispersion (2) [$W=6t$ denotes the bare bandwidth]. Dotted lines give the DOS of the two ζ-subbands. At optimal doping $x\simeq 0.3$, the chemical potential $\mu_0\equiv\mu(T=0)$ is located near the lower maximum of the DOS.

A. Delocalized Zener state

The degeneracy of the e_g states in (cubic) manganese oxides implies that the itinerant e_g electrons carry an orbital degree of freedom, namely, $\theta=|3z^2-r^2\rangle$ and $\epsilon=|x^2-y^2\rangle$ (remember that the Jahn-Teller distortion, lifting the e_g degeneracy, vanishes in the highly doped low-temperature metallic phase). Consequently the e_g electron transfer amplitude between neighboring Mn sites is anisotropic and depends on the orbital orientation,[62,63]

$$t^{x/y}_{\alpha\beta}=\frac{t}{4}\begin{bmatrix}1 & \mp\sqrt{3}\\ \mp\sqrt{3} & 3\end{bmatrix},\quad t^{z}_{\alpha\beta}=t\begin{bmatrix}1 & 0\\ 0 & 0\end{bmatrix} \tag{1}$$

with $\alpha,\beta\in\{\theta,\epsilon\}$. The orbital pseudospin is not a conserved quantity. If we neglect on-site Coulomb repulsion for the moment, the dispersion of the corresponding (noninteracting) two-band ($\zeta=\pm$) tight-binding Hamiltonian is given by

$$\begin{aligned}\varepsilon^{(0)}_{\mathbf{k}\zeta}=-t[&\cos k_x+\cos k_y+\cos k_z\pm(\cos^2 k_x+\cos^2 k_y\\&+\cos^2 k_z-\cos k_x\cos k_y-\cos k_y\cos k_z\\&-\cos k_z\cos k_x)^{1/2}].\end{aligned} \tag{2}$$

This band structure yields the density of states (DOS) depicted in Fig. 1 (cf. also Ref. 28). Although the results will not change dramatically using an (isotropic) simple cubic or even constant DOS, we employ this anisotropic DOS for all

the calculations presented below. However, to account for the strong Hund's rule and large on-site Hubbard interaction ($U \gg J_H \gg t_{\alpha\beta}^{x/y/z}$ reflects the situation in the manganites[64,65]), we insert some modifications. On one hand, the (two-band) DOS in Fig. 1 is normalized to one to prevent double occupied sites. This leads to an additional prefactor 1/2 in all $(\mathbf{k},\zeta)$ summations. On the other hand, combining the action of the Zener double exchange with the percolative approach, the bandwidth of the Zener state is renormalized, leading to the effective hole band

$$\overline{\varepsilon}_{\mathbf{k}\zeta} = p^{(f)} \gamma_{\overline{S}}[\overline{S}\lambda] \varepsilon_{\mathbf{k}\zeta}^{(0)}. \tag{3}$$

That is, in our model the renormalization of the band energy of the Zener state is driven by two mechanisms.

At first, introducing an effective field $\lambda = \beta g \mu_B H_{\mathrm{eff}}^z$ that tends to order the ion spins in the z direction, we have the temperature- and field-dependent band narrowing due to the Kubo-Ohata factor[9]

$$\gamma_{\overline{S}}[z] = \frac{1}{2} + \frac{\overline{S}}{2\overline{S}+1} \coth\left(\frac{2\overline{S}+1}{2\overline{S}} z\right) \times \left[\coth(z) - \frac{1}{2\overline{S}} \coth\left(\frac{z}{2\overline{S}}\right)\right]. \tag{4}$$

Here $\overline{S} = S + 1/2$ refers to the total $3d$ spin of an Mn^{3+} ion when an e_g electron is present, and $S = 3/2$ is the total core spin formed by the three t_{2g} electrons. This factor (4), yielding an effective hole transfer amplitude

$$\tilde{t} = \gamma_{\overline{S}}[\overline{S}\lambda] t, \tag{5}$$

was obtained averaging the transfer matrix element for a single nearest-neighbor Mn^{3+}-Mn^{4+} bond over all values and directions of the total bond spin S_T (cf. Refs. 9 and 16).

Next, the percolative aspects of the metal-insulator transition discussed above imply that, at least just above x_c (critical concentration for the occurrence of the FM metallic state at $T=0$) or below T_c, there exist insulating (polaronic) enclaves sparsely embedded in the conducting FM (Zener) phase. Thus the FM phase occupies a volume smaller than the sample volume, i.e., $N^{(f)} < N$, where N is the total number of sites and $N^{(f)}$ denotes the number of ions in the FM phase. Of course the sizes and shapes of the insulating microscopic islands are difficult to access quantitatively. For simplicity, within our two-fluid approach, we assume that the effective hole hopping amplitude has the value $\tilde{t}$ inside the conducting region [corresponding to the effective transport Hamiltonian (28) of previous work[16]] and zero elsewhere. Using Fourier analysis, the homogeneous component of this spatially dependent hopping amplitude, $\overline{t} = (N^{(f)}/N)\tilde{t}$, gives the renormalization of the bandwidth, whereas the long-wavelength Fourier components cause the scattering of the carriers. Naturally the size of the FM region, or equivalently the ''probability''

$$p^{(f)} = \frac{N^{(f)}}{N}, \tag{6}$$

has to be determined self-consistently (see Sec. II C). This introduces a *feedback effect*. Additional justification for the assumed reduction of the bandwidth proportional to the fraction of the FM region can be obtained from the numerical calculation of the density of states outlined in the Appendix for a simple tight-binding site percolation model without feedback.

B. Localized polaronic state

Let us denote the number of ions and localized electron vacancies (holes) in the polaronic phase by $N^{(p)}$ and $N_h^{(p)}$, respectively. Of course, $N^{(p)} = N - N^{(f)}$ and $N_h^{(p)} = N_h - N_h^{(f)}$ hold, where N_h is the total number of holes, i.e., $x = N_h/N$. Then the energy gain due to the Jahn-Teller splitting on localized electron sites without the influence of vacancies is weakened according to $(N^{(p)} - N_h^{(p)})E_1 = (x^{-1}-1)E_1 N_h^{(p)}$, where E_1 describes an effective Jahn-Teller energy in the polaronic regions. At the same time, if a doped hole is localized at a certain site, forming a small polaron, a breathing distortion may occur that lowers the energy of the unoccupied e_g level by the familiar polaron shift $E_p = -g^2\omega_0$ (see, e.g., Ref. 66), relative to its energy in an ideal structure. In addition, a reduction of the Jahn-Teller distortions in the neighborhood of the localized electron vacancy takes place. Both effects add up to an effective polaron binding energy $E_2 < 0$ per hole. Neglecting the exponentially small polaronic bandwidth, the polaronic phase, realized only in a fraction $p^{(p)} = N^{(p)}/N$ of the sample, can be represented approximately by spinless fermions (holes) having the site-independent energy

$$\varepsilon_p = (x^{-1}-1)E_1 + E_2. \tag{7}$$

As follows from a fitting of the resistivity data to a small polaron model,[33] in the region $0.2 < x < 0.5$, the x dependence of the parameter E_2 is rather weak, and therefore has been omitted in Eq. (7).

C. Self-consistency equations

The basic assumption of our mixed-phase scenario is the coexistence of metallic and insulating clusters with equal hole density, i.e., in accordance with recent experimental results[60,32] (see also Ref. 56), we assume that there is no large-scale separation of Mn^{3+} and Mn^{4+} ions in the CMR doping regime. This means

$$x = \frac{N_h}{N} = \frac{N_h^{(f)}}{N^{(f)}} = \frac{N_h^{(p)}}{N^{(p)}}, \tag{8}$$

but, of course, in general we have $N^{(f)} \neq N^{(p)}$ and $p^{(f)} \neq p^{(p)}$.

Denoting by $\langle \mathcal{H} \rangle$ the energy of the entire two-phase system within mean-field approximation and by $\mathcal{S}$ the corresponding entropy, $\mathcal{F} = \langle \mathcal{H} \rangle - T\mathcal{S}$ is an upper bound for the free energy. Introducing the grand-canonical potentials

$$\Omega^{(f)} = -\frac{1}{2\beta} \sum_{\mathbf{k},\zeta=\pm} \ln[1 + e^{\beta(\mu - \overline{\varepsilon}_{\mathbf{k}\zeta})}] \tag{9}$$

and

$$\Omega^{(p)} = -\frac{N}{\beta}\ln[1+e^{\beta(\mu-\varepsilon_p)}] \tag{10}$$

for holes in the FM and polaronic phases, respectively,

$$\mathcal{F} = N_h\mu + \Omega^{(f)} + \Omega^{(p)} - T\mathcal{S}^{(s)} \tag{11}$$

results, where

$$\begin{aligned}\mathcal{S}^{(s)} = k_B N[&p^{(f)}((1-x)(\ln \nu_{\bar{S}}[\bar{S}\lambda] - \lambda \bar{S} B_{\bar{S}}[\bar{S}\lambda]) \\ &+ x\{\ln \nu_S[S\lambda] - \lambda S B_S[S\lambda]\}) + p^{(p)}\{(1-x)\ln \nu_{\bar{S}}[0] \\ &+ x \ln \nu_S[0]\}]\end{aligned} \tag{12}$$

represents the mean-field ion-spin entropy, and

$$\nu_{\bar{S}}[z] = \sinh(z)\coth\left(\frac{z}{2\bar{S}}\right) + \cosh(z), \tag{13}$$

$$B_{\bar{S}}[z] = \frac{2\bar{S}+1}{2\bar{S}}\coth\left(\frac{2\bar{S}+1}{2\bar{S}}z\right) - \frac{1}{2\bar{S}}\coth\left(\frac{z}{2\bar{S}}\right). \tag{14}$$

If we use, instead of the model (28), the spin-dependent transport Hamiltonian (29) of our previous work,[16] assuming that the correlations of the spin background change on a time scale that is large compared with the hole hopping frequency, i.e., if we replace the effective hopping amplitude (5) by

$$\tilde{t}_{\downarrow} = \frac{\{\bar{S}(1+B_{\bar{S}}[\bar{S}\lambda])\}^2}{(2\bar{S})(2\bar{S}+1)}t, \tag{15}$$

the ion-spin entropy takes the form

$$\mathcal{S}^{(s)} = k_B N\{p^{(f)}(\ln \nu_{\bar{S}}[\bar{S}\lambda] - \lambda \bar{S} B_{\bar{S}}[\bar{S}\lambda]) + p^{(p)} \ln \nu_{\bar{S}}[0]\}. \tag{16}$$

At given temperature T and doping level x, *both* the ordering field for the FM state (λ) and the size of the Zener phase ($N^{(f)}$, or alternatively the hole fraction $N_h^{(f)}$) have to be determined in a *self-consistent* way, minimizing the free energy (11) on the hyperplane $\mu(\lambda, N^{(f)})$ given by

$$x = \frac{1}{2N}\sum_{\mathbf{k}\zeta}\frac{1}{e^{\beta(\varepsilon_{\mathbf{k}\zeta}-\mu)}+1} + \frac{1}{e^{\beta(\varepsilon_p-\mu)}+1}. \tag{17}$$

After that, the magnetization (more exact the averaged spin z component) can be calculated from

$$M = (1-x)\bar{S}p^{(f)}B_{\bar{S}}[\bar{S}\lambda] + xSp^{(f)}B_S[S\lambda]. \tag{18}$$

III. NUMERICAL RESULTS AND DISCUSSION

The changes in magnetization as a function of temperature are shown in Fig. 2 for different doping levels. The efficiency of the feedback effect is quite obvious. Omitting the $p^{(f)}$ factor in Eq. (3), a rather smooth variation of $M(T)$ results and the critical temperatures for the disappearance of the Zener state, $T_c(x)$, are too high as compared with the experimentally observed ones. Combining percolative and double-exchange mechanisms, within our simple two-phase model T_c is reduced substantially. The magnetization always exhibits a first-order transition, which reflects the behavior in $La_{1-x}Ca_xMnO_3$. On the other hand, $La_{1-x}Sr_xMnO_3$ shows a second-order phase transition,[67] but the drop of $M(T)$ at T_c is very abrupt. It can be expected that the inclusion of a small but finite polaron bandwidth [instead of the localized level (7)], softens the abrupt transition to some extent but in any case we will find a rather sharp transition.

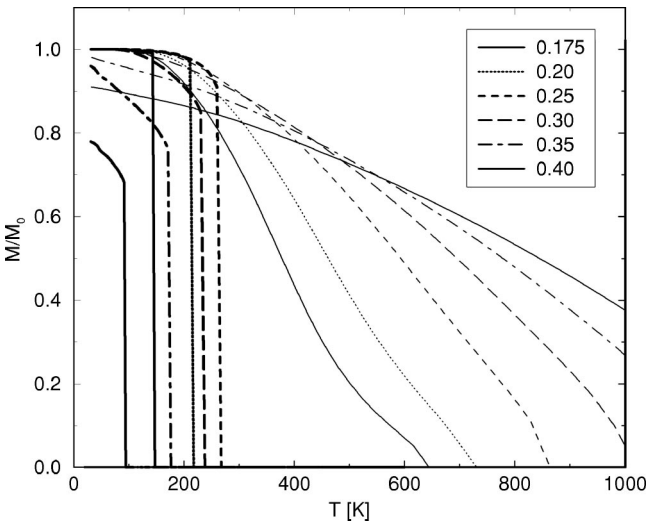

FIG. 2. Magnetization M, normalized by $M_0 = \bar{S} - x/2$, as a function of temperature T at various doping levels $x = 0.175, \ldots, 0.4$. Results are shown for the models with (bold lines) and without (thin lines) feedback using parameters $E_1 = -0.125$ eV, $E_2 = -0.25$ eV, and $W = 3.6$ eV.

Naturally the bandwidth of charge carriers in the Zener

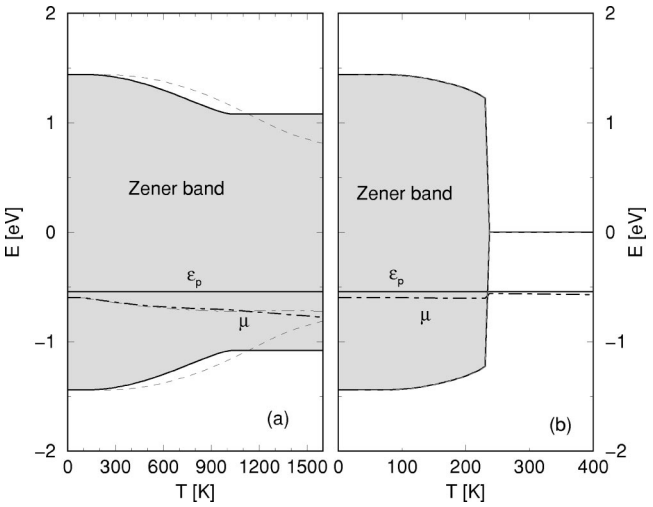

FIG. 3. Temperature dependences of the Zener band (shaded region) and of the positions of the polaronic level ε_p and chemical potential μ (a) without and (b) with feedback. Results are presented at $x = 0.3$ ($E_1 = -0.125$ eV, $E_2 = -0.25$ eV; $W = 3.6$ eV). Dashed lines display the band edges resulting from Eq. (15) instead of Eq. (5).

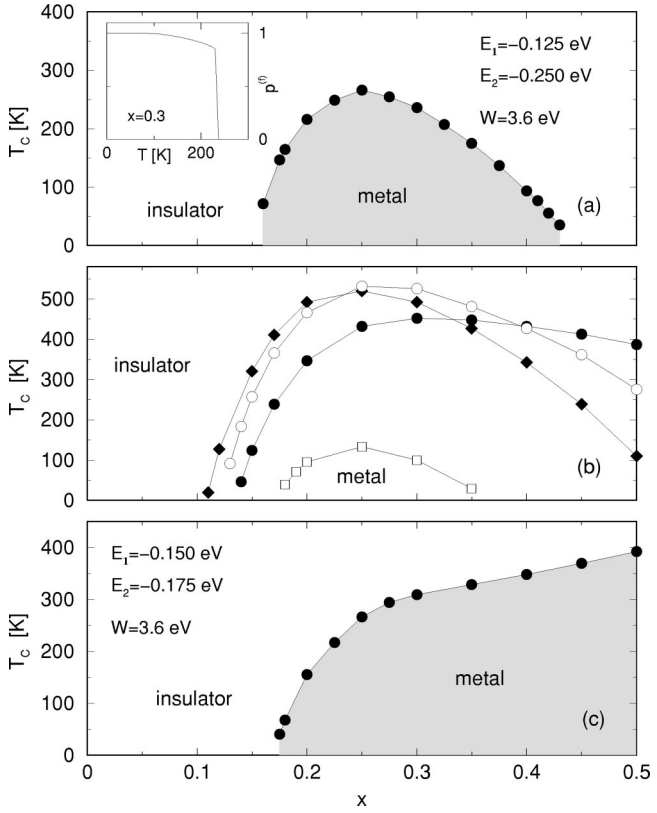

FIG. 4. Phase diagram of the mixed-phase Zener-polaron model with feedback. The inset of (a) shows the fraction of the Zener phase as a function of temperature. In panel (b), the parameter sets (E_1, E_2, W) in eV are filled circles $(-0.125, -0.2, 3.6)$, filled diamonds $(-0.1, -0.25, 3.6)$, open circles $(-0.125, -0.25, 4.0)$, and open squares $(-0.125, -0.25, 3.4)$.

state, displayed in Fig. 3 for a doping level $x=0.3$, reflects the behavior of the magnetization. Without feedback we found a moderate band narrowing, whereas a radical shrinking occurs in the feedback model, which can be traced back to the collapse of the FM metallic region at T_c. The use of the spin-dependent hopping amplitude (15) leads to a modification of the bandwidth (and μ) only for the scenario without feedback. Here, temperature-independent band edges correspond to complete spin disorder. Including the $p^{(f)}$ factor, both models (15) and (5) yield nearly identical results, which again indicates the dominance of the percolative feedback mechanism.

Figure 4 presents the central result of our work, the x-T phase diagram of the percolative two-phase model. It is clearly beyond the scope of the present approach to account for the complete phase diagram of real manganites, which contains a great variety of charge-, spin-, and orbital-ordered states. The focus is on the doping region $0.15<x<0.5$, where at low temperatures a band-description seems to be appropriate. In this regime, the phase diagrams of Figs. 4(a) and 4(c), determined for some characteristic parameter sets, describe the major features of the metal-insulator transition lines in $La_{1-x}Ca_xMnO_3$ and $La_{1-x}Sr_xMnO_3$.[68] Furthermore, the absolute values of the critical concentration $x_c(T=0) \simeq 0.17$ and of the transition temperatures T_c agree surprisingly well with the experimental data. A comparison of panels 4(a), 4(b), and 4(c) shows that the magnitude of T_c at high doping is mainly determined by E_2, which accounts for breathing polaron effects. This is in qualitative agreement with PDF experiments,[32,43] which indicate that the polarons in highly doped $La_{1-x}Ca_xMnO_3$ are rather of the conventional breathing type. Moreover, the dependence on E_2 is consistent with optical measurements[36] pointing towards a stronger electron-phonon coupling in $La_{1-x}Ca_xMnO_3$ as compared to $La_{1-x}Sr_xMnO_3$. On the other hand, the value of $x_c(T=0) \simeq 0.17$, which in our theory is mainly controlled by E_1, in real materials is certainly also affected by other mechanisms, such as orbital and superexchange interactions[69] or changes of the lattice structure.[70] As can be seen from panel 4(b), the phase boundary strongly depends on the bare bandwidth W. Clearly larger W promotes double exchange and therefore enhances the metallic region. Note that the above values of W are consistent with estimates of the bare bandwidth from kinetic energy.[71]

As illustrated with the inset in Fig. 4(a), the low-temperature phase contains, besides the FM metallic region, finite domains of the localized polaronic phase ($p^{(f)}<1$, and accordingly $p^{(p)}>0$), the fraction of which increases with increasing temperature. At T_c, there is an abrupt spill-over of holes between the delocalized and localized phases, which drives the metal-insulator transition. Since the conductivity is proportional to the number of delocalized holes $N_h^{(f)}$, a dramatic change at T_c results. In the insulating high-temperature phase, the band description breaks down, and the transport properties are dominated by incoherent small polaron hopping processes. For doping levels $x<x_c$, the system behaves as a FM insulator with short-range polaronic correlations.[46]

IV. SUMMARY

Although the theoretical understanding of the CMR phenomenon is still incomplete, double-exchange, electron-phonon, and orbital effects are commonly accepted as the main ingredients. Based on an in-depth analysis of important new experimental information about the inhomogeneous microscopic structure of the FM metallic state, we come to the conclusion that in addition mixed-phase tendencies and percolative behavior play an important role in doped manganites, in particular in the vicinity of the metal-insulator transition. To simulate these effects, we have studied a simple semiphenomenological model, describing coexisting polaronic insulating and double-exchange-dominated metallic phases with equal hole density. The fraction of localized and delocalized states was determined self-consistently. Below the transition temperature T_c, we found polaronic inclusions embedded in a dominant macroscopic metallic phase. Our approach, which is distinct from that of the electronic phase separation concept involving states with different carrier density, provides an alternative explanation of the FM metal to polaronic insulator transition. The abrupt change, revealed in various electrical and magnetic properties at T_c, was attributed to a collapse of the Zener state mainly caused by a percolative feedback mechanism. At $T=0$ the transition is

driven by doping and occurs at $x_c \simeq 0.15$–0.18. At finite temperatures, disorder due to intrinsic inhomogeneities and magnetic scattering act in combination to reduce the mobility of the charge carriers. The calculated values of T_c agree fairly well with the experimental ones. In conclusion, we believe that a further elaboration of the proposed percolative mixed-phase scenario, e.g., towards a direct calculation of the transport properties, may help to clarify many puzzling aspects of the CMR compounds.

ACKNOWLEDGMENTS

The authors are greatly indebted to L. F. Feiner, R. Kilian, and A. M. Oleś for stimulating discussions and helpful comments. This work was supported by the Deutsche Forschungsgemeinschaft and the Czech Academy of Sciences under Grant No. 436 TSE 113/33.

APPENDIX: PERCOLATIVE PICTURE

To support the assumption that the width of the conduction band depends approximately linearly on the fraction of the FM region [see Sec. II A, Eq. (3)], let us consider a site percolation model on a finite hypercubic lattice with 64^3 sites and periodic boundary conditions. The lattice points are occupied with probability p. Adjacent occupied sites will be connected by a hopping matrix element. The density of states of the resulting random tight-binding model,

$$\mathcal{H}_p = \sum_{\langle ij \rangle} t_p (c_i^\dagger c_j + c_j^\dagger c_i), \tag{A1}$$

$t_p \in \{0,1\}$, is determined numerically in two different ways, using kernel polynomial and maximum entropy methods.[72,73] On the one hand, we start from a single realization $\mathcal{H}_p$ and determine 400 Chebyshev moments of $\mathcal{H}_p$ using 100 random start vectors. On the other hand, we use 10 realizations of $\mathcal{H}_p$ and compute for each realization 200 moments from 50 random start vectors. The results basically agree.

Figure 5 displays the (averaged) density of states for various values of p. Self-evidently, p now is simply a model parameter, i.e., there is no feedback effect as considered in Sec. II A. A significant change of the spectrum around the site percolation threshold, $p_c \simeq 0.31$, is observed. Below p_c, the DOS is mainly confined to the interval $[-2,2]$, as for a one-dimensional model, and mostly consists of isolated peaks with different spectral weight. This can be seen more clearly from the steplike behavior of the integrated density of states, $N(E) = \int_{-W/2}^{E} \mathrm{DOS}(E')dE'$, shown in the lower panel. The steps can be attributed to metallic ''islands'' (finite clusters) containing delocalized electrons. They form a cluster comparable to the system size first at $p = p_c$. Above

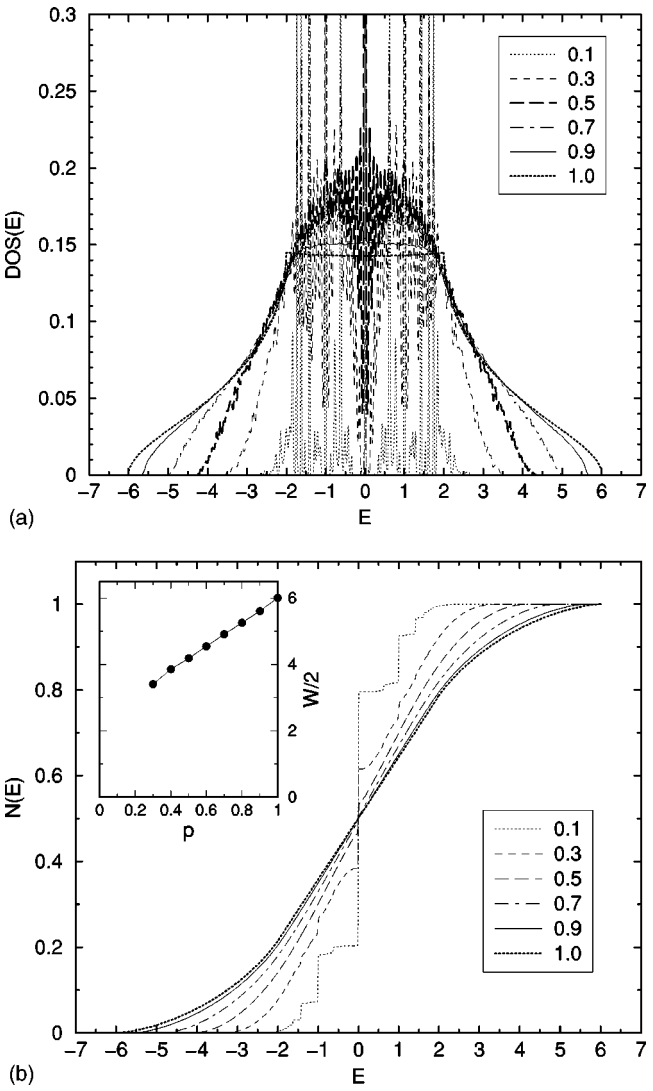

FIG. 5. Density of states (DOS) (upper panel) and integrated DOS $[N(E)]$ for the tight-binding site percolation model with different probabilities $p = 0.1, 0.3, \ldots, 1$. The inset gives the bandwidth as a function of p.

p_c, $N(E)$ becomes a continuous function and the DOS is evocative of that of a simple cubic tight-binding model but with a reduced bandwidth. That is, although the percolative cluster occupies most of the bulk, making the whole system metallic, smaller conducting and insulating regions are embedded into it. These enclaves act as small scattering centers, causing the band narrowing. The inset demonstrates the almost perfect linear dependence of W on p, in particular at large p, which in reality is the region of interest (cf. the inset of Fig. 4).

[1] S. Jin, T. H. Tiefel, M. McCormack, R. A. Fastnach, R. Ramesh, and L. H. Chen, Science **264**, 413 (1994).
[2] G. H. Jonker and J. H. van Santen, Physica (Amsterdam) **16**, 337 (1950); J. H. van Santen and G. H. Jonker, *ibid.* **16**, 599 (1950).
[3] Y. Tokura and Y. Tomioka, J. Magn. Magn. Mater. **200**, 1 (1999).
[4] J. M. D. Coey, M. Viret, and S. von Molnar, Adv. Phys. **48**, 167 (1999).
[5] E. Dagotto, T. Hotta, and A. Moreo, Phys. Rep. **344**, 1 (2001).
[6] C. Zener, Phys. Rev. **82**, 403 (1951).
[7] P. W. Anderson and H. Hasegawa, Phys. Rev. **100**, 675 (1955).

[8] P.-G. de Gennes, Phys. Rev. **118**, 141 (1960).
[9] K. Kubo and N. Ohata, J. Phys. Soc. Jpn. **33**, 21 (1972).
[10] P. Schiffer, A. P. Ramirez, W. Bao, and S.-W. Cheong, Phys. Rev. Lett. **75**, 3336 (1995).
[11] A. P. Ramirez, P. Schiffer, S.-W. Cheong, C. H. Chen, W. Bao, T. T. M. Palstra, P. L. Gammel, D. J. Bishop, and B. Zegarski, Phys. Rev. Lett. **76**, 3188 (1996).
[12] A. J. Millis, P. B. Littlewood, and B. I. Shraiman, Phys. Rev. Lett. **74**, 5144 (1995).
[13] A. Moreo, S. Yunoki, and E. Dagotto, Science **283**, 2034 (1999).
[14] A. J. Millis, Nature (London) **392**, 147 (1998).
[15] A. S. Alexandrov and A. M. Bratkovsky, Phys. Rev. Lett. **82**, 141 (1999).
[16] A. Weiße, J. Loos, and H. Fehske, Phys. Rev. B **64**, 054406 (2001).
[17] M. E. Fisher and J. S. Langer, Phys. Rev. Lett. **20**, 665 (1968).
[18] P. Majumdar and P. B. Littlewood, Nature (London) **395**, 479 (1998).
[19] S. Ishihara, M. Yamanaka, and N. Nagaosa, Phys. Rev. B **56**, 686 (1997).
[20] R. Kilian and G. Khaliullin, Phys. Rev. B **58**, R11 841 (1998).
[21] P. Horsch, J. Jaclič, and F. Mack, Phys. Rev. B **59**, 6217 (1999).
[22] M. S. Laad, L. Craco, and E. Müller-Hartmann, Phys. Rev. B **63**, 214419 (2001).
[23] A. M. Oleś, M. Cuoco, and N. B. Perkins, in *Lectures on the Physics of Highly Correlated Electron Systems IV*, AIP Conf. Proc. No. 527, edited by F. Mancini (AIP, New York, 2000), p. 226–380.
[24] A. J. Millis, B. I. Shraiman, and R. Müller, Phys. Rev. Lett. **77**, 175 (1996).
[25] H. Röder, J. Zhang, and A. R. Bishop, Phys. Rev. Lett. **76**, 1356 (1996).
[26] G. Zhao, K. Conder, H. Keller, and K. A. Müller, Nature (London) **381**, 676 (1996).
[27] N. A. Babushkina, L. M. Belova, O. Y. Gorbenko, A. R. Kaul, A. A. Bosak, V. I. Ozhogin, and K. I. Kugel, Nature (London) **391**, 159 (1998).
[28] R. Kilian, Ph.D. thesis, Technische Universität Dresden (1999).
[29] M. D. Sturge, *Solid State Physics*, edited by F. Seitz, D. Turnbull, and H. Ehrenreich (Academic, New York, 1967), Vol. 20, p. 91.
[30] J. R. Fletcher and K. W. H. Stephens, J. Phys. C **2**, 444 (1969).
[31] P. B. Allen and V. Perebeinos, Phys. Rev. B **60**, 10 747 (1999).
[32] S. J. L. Billinge, T. Proffen, V. Petkov, J. L. Sarrao, and S. Kycia, Phys. Rev. B **62**, 1203 (2000).
[33] D. C. Worledge, L. Miéville, and T. H. Geballe, Phys. Rev. B **57**, 15 267 (1998).
[34] P. Calvani, P. Dore, S. Lupi, A. Paolone, P. Maselli, P. Guira, B. Ruzicka, S.-W. Cheong, and W. Sadowski, J. Supercond. **10**, 293 (1997).
[35] J. D. Lee and B. I. Min, Phys. Rev. B **55**, 12 454 (1997).
[36] M. Quijada, J. Černe, J. R. Simpson, H. D. Drew, K. H. Ahn, A. J. Millis, R. Shreekala, R. Ramesh, M. Rajeswari, and T. Venkatesan, Phys. Rev. B **58**, 16 093 (1998).
[37] K. H. Kim, J. H. Jung, and T. W. Noh, Phys. Rev. Lett. **81**, 1517 (1998).
[38] K. A. Müller, J. Supercond. **12**, 3 (1999).
[39] D. S. Dessau, T. Saitoh, C.-H. Park, Z.-X. Shen, P. Villella, N. Hamada, Y. Morimoto, and Y. Tokura, J. Supercond. **12**, 273 (1999).
[40] M. Jaime, M. B. Salamon, M. Rubinstein, R. E. Treece, J. S. Horowitz, and D. B. Chrisey, Phys. Rev. B **54**, 11 914 (1996).
[41] T. T. M. Palstra, A. P. Ramirez, S.-W. Cheong, B. R. Zegarski, P. Schiffer, and J. Zaanen, Phys. Rev. B **56**, 5104 (1997).
[42] M. Jaime, H. T. Hardner, M. B. Salamon, M. Rubinstein, P. Dorsey, and D. Emin, Phys. Rev. Lett. **78**, 951 (1997).
[43] S. J. L. Billinge, R. G. DiFrancesco, G. H. Kwei, J. J. Neumeier, and J. D. Thompson, Phys. Rev. Lett. **77**, 715 (1996).
[44] S. Shimomura, N. Wakabayashi, H. Kuwahara, and Y. Tokura, Phys. Rev. Lett. **83**, 4389 (1999).
[45] L. Vasiliu-Doloc, S. Rosenkranz, R. Osborn, S. K. Sinha, J. W. Lynn, J. Mesot, O. H. Seeck, G. Preosti, A. J. Fedro, and J. F. Mitchell, Phys. Rev. Lett. **83**, 4393 (1999).
[46] P. Dai, J. A. Fernandez-Baca, N. Wakabayashi, E. W. Plummer, Y. Tomioka, and Y. Tokura, Phys. Rev. Lett. **85**, 2553 (2000).
[47] D. Louca, T. Egami, E. L. Brosha, H. Röder, and A. R. Bishop, Phys. Rev. B **56**, R8475 (1997).
[48] G. M. Zhao, V. Smolyaninova, W. Prellier, and H. Keller, Phys. Rev. Lett. **84**, 6086 (2000).
[49] A. Lanzara, N. L. Saini, M. Brunelli, F. Natali, A. Bianconi, P. G. Radaelli, and S.-W. Cheong, Phys. Rev. Lett. **81**, 878 (1998).
[50] C. H. Booth, F. Bridges, G. H. Kwei, J. M. Lawrence, A. L. Cornelius, and J. J. Neumeier, Phys. Rev. Lett. **80**, 853 (1998).
[51] S. Yunoki, A. Moreo, and E. Dagotto, Phys. Rev. Lett. **81**, 5612 (1998).
[52] M. Fäth, S. Freisem, A. A. Menovsky, Y. Tomioka, J. Aarts, and J. A. Mydosh, Science **285**, 1540 (1999).
[53] M. Uehara, S. Mori, C. H. Chen, and S.-W. Cheong, Nature (London) **399**, 560 (1999).
[54] L. P. Gor'kov and V. Z. Kresin, Pis'ma Zh. Éksp. Teor. Fiz. **67**, 834 (1998) [JETP Lett. **67**, 985 (1998)].
[55] L. P. Gor'kov and V. Z. Kresin, J. Supercond. **12**, 243 (1999).
[56] A. Moreo, M. Mayr, A. Feiguin, S. Yunoki, and E. Dagotto, Phys. Rev. Lett. **84**, 5568 (2000).
[57] S. J. L. Billinge and T. Egami, Phys. Rev. B **47**, 14 386 (1993).
[58] V. Chechersky, A. Nath, I. Isaac, J. P. Franck, K. Ghosh, H. Ju, and R. L. Greene, Phys. Rev. B **59**, 497 (1999).
[59] J. W. Lynn, R. W. Erwin, J. A. Borchers, Q. Huang, A. Santoro, J.-L. Peng, and Z. Y. Li, Phys. Rev. Lett. **76**, 4046 (1996).
[60] R. H. Heffner, J. E. Sonier, D. E. MacLaughlin, G. J. Nieuwenhuys, G. Ehlers, F. Mezei, S.-W. Cheong, J. S. Gardner, H. Röder, Phys. Rev. Lett. **85**, 3285 (2000); R. H. Heffner, J. E. Sonier, D. E. MacLaughlin, G. J. Nieuwenhuys, G. M. Luke, Y. J. Uemura, W. Ratcliff, S.-W. Cheong, and G. Balakrishnan, Phys. Rev. B **63**, 094408 (2001).
[61] In an alternative description, the manganites were considered as charge-transfer-type insulators with carriers mainly residing on oxygen *p* orbitals. In this scenario, the ferromagnetism is caused by *d*-*p* exchange and strong electron-phonon coupling [see Ref. 15, or G. Zhao, Phys. Rev. B **62**, 11 639 (2000)]
[62] J. C. Slater and G. F. Koster, Phys. Rev. **94**, 1498 (1954).
[63] K. I. Kugel and D. I. Khomskii, Zh. Éksp. Teor. Fiz. **64**, 1429 (1973) [Sov. Phys. JETP **37**, 725 (1973)].
[64] A. E. Bocquet, T. Mizokawa, T. Saitoh, H. Namatame, and A. Fujimori, Phys. Rev. B **46**, 3771 (1992); J. Zaanen and G. A. Sawatzky, J. Solid State Chem. **88**, 8 (1990); T. Mizokawa and A. Fujimori, Phys. Rev. B **51**, 12 880 (1995).
[65] In the doping region considered in the present work ($0.2 \leqslant x \leqslant 0.5$), double exchange is the leading magnetic interaction, in

particular the ferro- and antiferromagnetic superexchange interactions are much less important (see, e.g., Ref. 69).

[66] H. Fehske, J. Loos, and G. Wellein, Phys. Rev. B **61**, 8016 (2000).

[67] J. Mira, J. Rivas, F. Rivadulla, C. Vázquez-Vázquez, and M. A. López-Quintela, Phys. Rev. B **60**, 2998 (1999).

[68] M. Imada, A. Fujimori, and Y. Tokura, Rev. Mod. Phys. **70**, 1039 (1998).

[69] Y. Endoh, K. Hirota, S. Ishihara, S. Okamoto, Y. Murakami, A. Nishizawa, T. Fukuda, H. Kimura, H. Nojiri, K. Kaneko, and S. Maekawa, Phys. Rev. Lett. **82**, 4328 (1999).

[70] Q. Huang, A. Santoro, J. W. Lynn, R. W. Erwin, J. A. Borchers, J. L. Peng, K. Ghosh, and R. L. Greene, Phys. Rev. B **58**, 2684 (1998).

[71] A. Chattopadhyay, A. J. Millis, and S. Das Sarma, Phys. Rev. B **61**, 10 738 (2000).

[72] R. N. Silver, H. Röder, A. F. Voter, and J. D. Kress, J. Comput. Phys. **124**, 115 (1996); R. N. Silver and H. Röder, Phys. Rev. E **56**, 4822 (1997).

[73] B. Bäuml, G. Wellein, and H. Fehske, Phys. Rev. B **58**, 3663 (1998).